Materials Physics and Mechanics 41 (2019) 62-68 Received: January 31, 2018

EFFECT OF ANODIC VOLTAGE ON PARAMETERS OF POROUS ALUMINA FORMED IN SULFURIC ACID ELECTROLYTES

X. Huang[1], W. Su[1], L. Sun[1], J. Liu[1], D.A. Sasinovich[2], O.V. Kupreeva[2], D.A. Tsirkunov[2], G.G. Rabatuev[2], S.K. Lazarouk[2*]

[1]Hangzhou Dianzi University, 310018, Hangzhou, China

[2]Belarusian State University of Informatics and Radioelectronics, P. Browka 6, 220013 Minsk, Belarus

*e-mail: serg@nano.bsuir.edu.by

Abstract. Local porous aluminum anodizing with a photolithography mask has been carried out at anodic voltages varying from 15 to 200 V in sulfuric acid electrolytes. Record anodic voltages at room temperature have been achieved leading to new parameters of porous alumina such as interpore distance up to 320 nm, forming cell factor up to 1.2 nm/V, thickness expansion factor up to 3.5, porosity up to 1%, sulfur concentration up to 7.7 at.%. A central angle of porous alumina cells has been measured in concave points as well as in peak points of porous alumina cells at the border with aluminum. The measurements have shown that central angles can reach 90° at anodic voltages larger than 100 V. The electric field distribution in porous alumina cells has been simulated for different central angles. It is found that the electric field reaches 2.7×10^{10} V/m in the layers with a porosity of 1% in growing alumina.

Keywords: combustion, explosion, mechanical pulse, microthruster, multichip structure, nanoporous silicon

1. Introduction

Porous aluminum anodizing provides formation of hexagonal alumina cells with pores in their centers. Porous alumina attracts much attention because of its self-ordered hexagonal structure with cell sizes depending on anodic voltage [1]. Self-ordering of alumina hexagonal cells during anodizing is considerably improved at high forming voltages [2]. Such an electrochemical process was called the high field anodizing and provided the fabrication of ordered porous alumina with tubular structures [3,4]. Porous alumina structure parameters include interpore distance, pore diameter, film thickness, volume (thickness) expansion factor and the central angle of the barrier layer in alumina hexagonal cells. Unfortunately, only a few papers are devoted to the investigation of the central angle [5,6]. Usually, central angle measurements have been performed between the center and concave point at the cell border. Angle measurements between a center and a point of the aluminum peak have not been made yet.

In this paper, the high voltage aluminum anodizing in sulfuric acid electrolytes is analyzed. The porous alumina parameters obtained at different anodic voltages up to 200 V have been studied. The special attention has been paid to studying the central angle in porous alumina hexagonal cells. The central angle has been measured in concave points as well as in peak points of porous alumina cells formed in a wide range of anodic voltages. The influence of the peak central angle on electric field distribution in porous alumina nanocells is discussed.

http://dx.doi.org/10.18720/MPM.4112019_9

2. Experimental

Aluminum foil (purity 99.9%) with the thickness of 100 μm and 1.0 μm thick aluminum films deposited on silicon wafers were used as initial samples. A 0.2 μm niobium film was deposited on the aluminum surface to form a mask. Then the niobium mask was configurated by standard photolithography operations and plasma-chemical etching in SF_6 gas. Porous aluminum anodizing was carried out in 0.2 M - 6.3 M H_2SO_4 aqueous solutions at room temperature. The anodizing voltage was linearly increased from 0 to 15200 V with a rate of 10 V/s.

The thickness expansion factor of the anodic oxide was calculated from the metal and oxide thickness measurements. The structure parameters of the anodic films were analyzed by a scanning electron microscopy (SEM) and transmission electron microscopy (TEM). The film porosity was estimated by using SEM and TEM measurements of the pore diameters and the interpore distances. Atomic composition of the samples was studied by Energy Dispersive X-Ray (EDX) analysis.

The electric field distribution has been calculated based on porous alumina cell structure parameters and anodic voltage used during anodizing process. The Comsol Multiphysics program complex has been used to solve Poisson's equation for a given configuration [5,7].

3. Results and discussion

Figure 1 shows a schematic view of aluminum porous anodizing with a photolithography mask indicating possible ways for Joule heat to disperse. It is evident that aluminum anodizing with a mask provides additional ways to heat dissipation. The heat sink through aluminum tracks and a niobium mask prevents overheating in the alumina barrier layer. This approach allows reaching the maximum forming voltage of 200 V for sulfuric electrolytes, whereas an ordinary full-area anodizing process can be carried out at the maximum forming voltage of about 70 V [2].

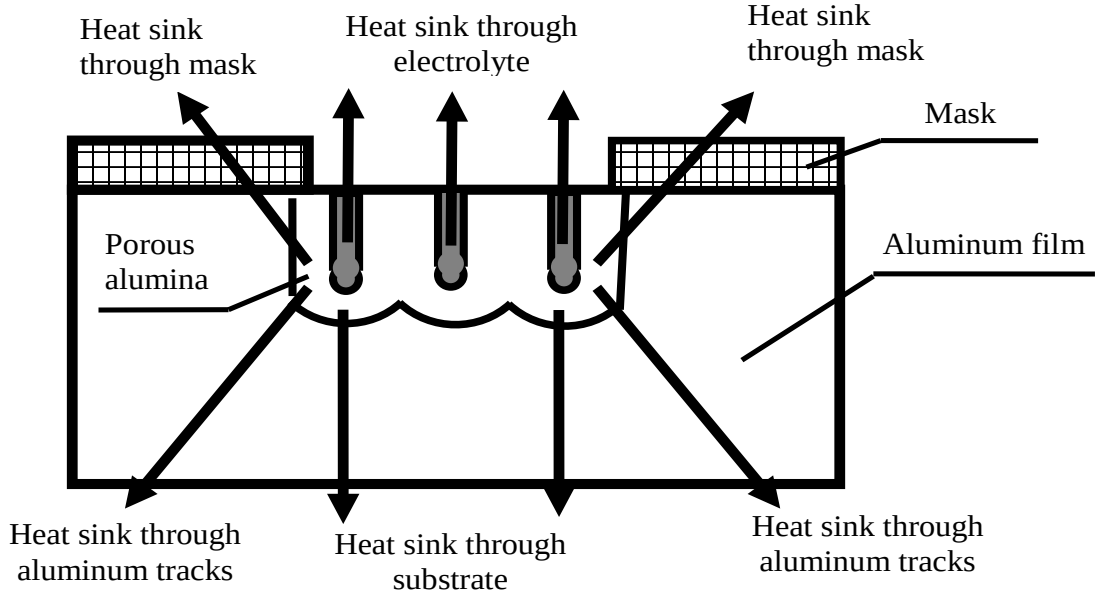

Fig. 1. The schematic view of heat sinks during porous aluminum anodizing with a photolithography fabricated mask

Porous alumina films include close-packed hexagonal alumina cells where each cell consists of a hexagonal prism with a cylindrical pore at the center and a barrier layer at the boundary with metallic surface (Fig. 2 a). The barrier layer is the space between the lower

base of hexagonal prism and a spherical surface at the border with aluminum. Such configuration provides the presence of peak points and concaves at the aluminum surface (Fig. 2 b, c). The barrier layer structure in porous alumina nanocells is characterized by the following parameters: interpore distance (*L*), pore diameter (*d*) and central angle (θ) (Fig. 2 a). The central angle is an angle which apex (vertex) is the center of a circle and whose legs are radii intersecting the circle in two distinct points. The first point is the center of spherical surface in the alumina cell. The second point can be chosen in metal peak points as well as in concave points (Fig. 2 b, c). Obviously, the peak central angle is larger with respect to concave one for the same hexagonal alumina cell. The simple calculation shows that the difference between peak and concave central angles can reach 50%. Therefore, the central angles for porous alumina cells should be specified as θ_{peak} and as $\theta_{concave}$.

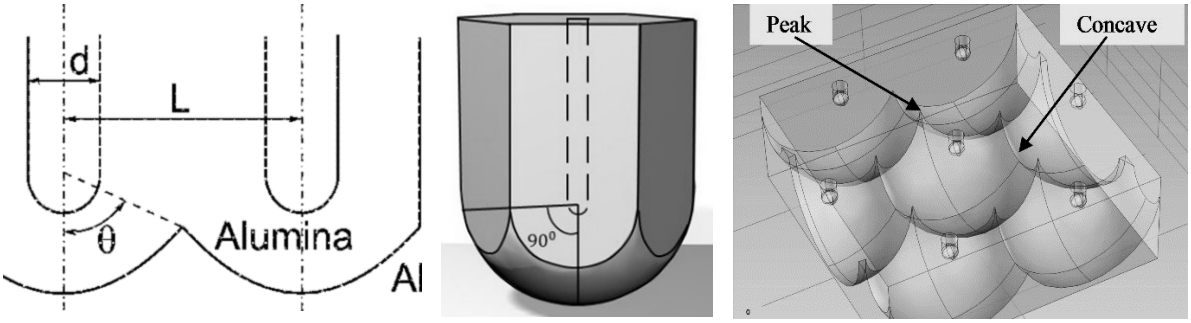

(*a*) (*b*) (*c*)

Fig. 2. Schematic view of porous alumina nanocells: *a)* cross-sectional view with the specified structure parameters; *b*) general view of porous alumina nanocell with the specified central angle in the peak point, *c*) general view of the spherical aluminum surface with a peak point and a concave point marked

Figure 3 shows SEM cross-section images of porous alumina formed at different anodic voltages in the range from 15 V up to 200 V. Porous alumina formed at 15 V has a "honey comb" structure and its cross section passes through pore centers (Fig. 3 a). The anodic films formed at 30 V and higher have a tubular structure and their cross sections pass through tube borders (Fig. 3 b-d). Further increase of anodic voltage is limited due to appearing local breakdown effects.

It results in microplasma glow visualized by optical microscopy (Fig. 4 a, inset). Microplasma causes inhomogeneity of porous alumina structure (Fig. 3 d). Figure 4 shows structure parameters of porous alumina *vs* anodic voltage. Its growth leads to increasing the distance between pore centers (interpore distance) up to 300 nm in the 6.3 M H_2SO_4 electrolyte (Fig. 4 a). The higher interpore distance for anodic films formed in 6.3 M H_2SO_4 electrolyte can be explained by lower electrolyte resistivity with respect to the 0.2 M H_2SO_4 electrolyte [8]. Formation cell factor (ratio between interpore distance and anodic voltage) decreases from 2.5 nm/V at $U_a = 20$ V to 1.2 nm/V at $U_a = 200$ V for the 0.2 M H_2SO_4 electrolyte. Thickness expansion factor increases up to 3.5 whereas porosity decreases to 1% with the anodic voltage growth.

EDX analysis has shown that the oxygen and aluminum concentration ratio is 1.4 for porous alumina formed at low anodic voltages while the same parameter is 3.5 for anodic films formed at 140 V. Besides the sulfur concentration increases from 1 up to 7.7 at.% with the anodic voltage growth. It means that porous alumina films formed at low anodic voltages consist of stoichiometric Al_2O_3 while anodic films formed at high anodic voltages consist of $Al(OH)_3 + Al_2O_3 + (SO_4)^{2-}$anion complexes as it was proposed in Ref. [3]. The thickness expansion factor data validate this assumption because the value of 3.5 corresponds to $Al \rightarrow Al(OH)_3$.

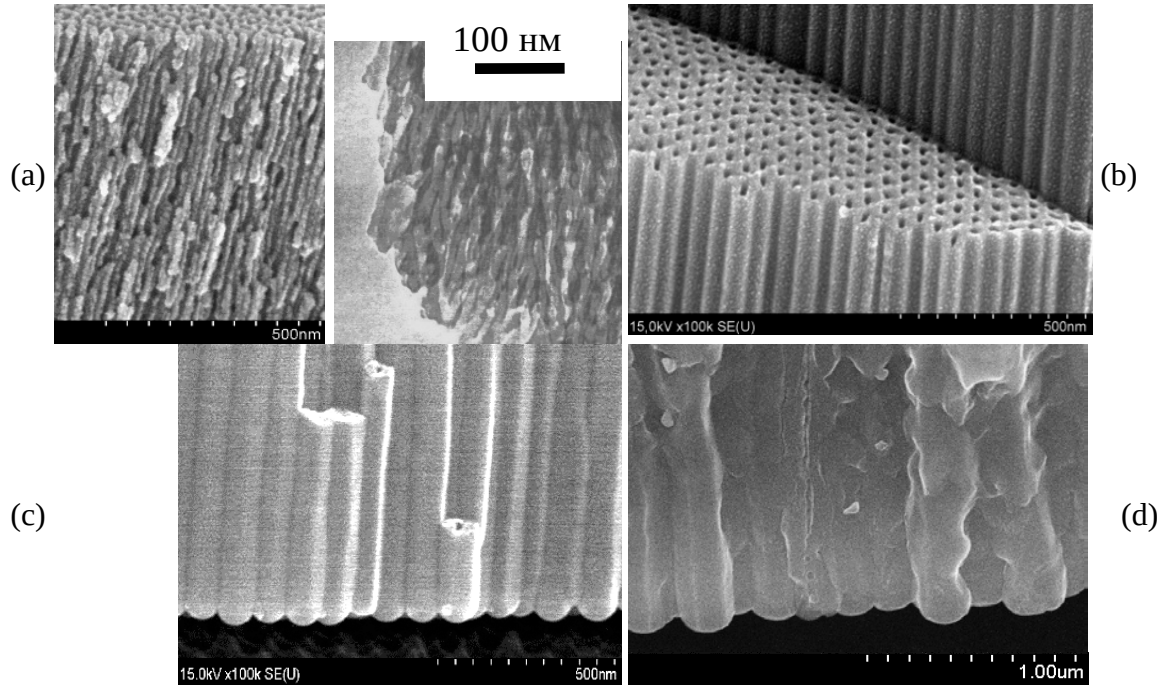

Fig. 3. SEM and TEM cross-section images of porous alumina formed at different anodic voltages: (a) 15, (b) 30, (c) 70, (d) 200 V

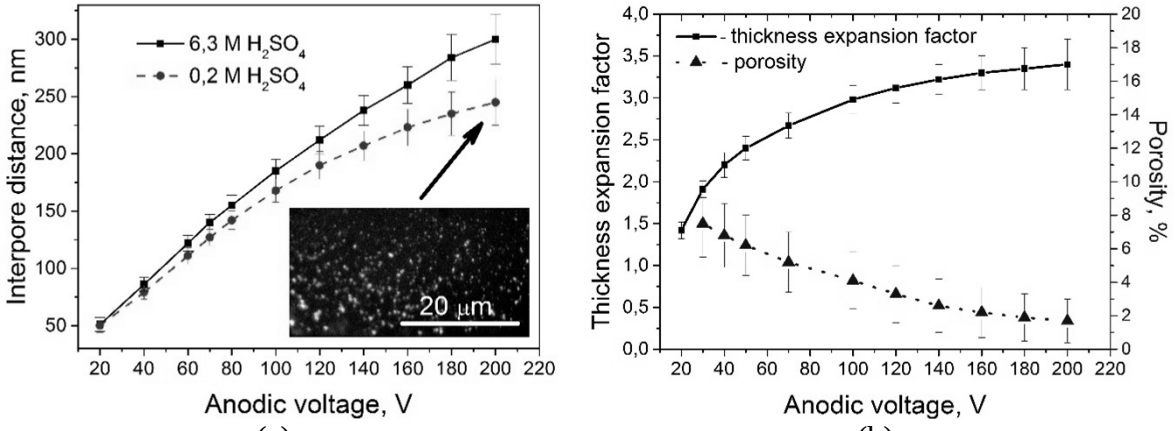

Fig. 4. Porous alumina structure parameters *vs* anodic voltage: a) interpore distance in porous alumina formed in different sulfuric acid electrolytes (photo of microplasmas at anodic voltage 200 V is shown in inset); b - thickness expansion factor and porosity

SEM images of porous alumina and aluminum surface are illustrated in Figure 5 a, b. Alumina tubes with a semispherical barrier layer are in the upper part of the photo (Fig. 5 a). Concave central angles were measured in spherical parts of porous alumina cells similar to the method in Refs. [5,6]. Peak central angles were measured on the aluminum surface relief (bottom part of the photo). As can be seen in SEM images (Fig. 5 a, b), peak central angles exceed concave central angles. The aluminum peaks have sharp forms. Their curvature radius is less than a few nanometers.

Figure 5 c exhibits peak central angles and concave central angles *vs* anodic voltage. The difference between the peak and concave angles is small for porous alumina formed at low anodic voltages. The central angles are increased with the anodic voltage growth.

The average peak central angles reached 90 deg whereas the average concave angles attained 60 deg for high anodic voltages.

Figure 6 presents the calculated electric field distribution in the porous alumina nanocells with different central angles. The cells have been formed at U_a=140 V. The maximum field strength appears at the pore bottom and near the aluminum peaks. With increasing the center angle, the electric field enhances.

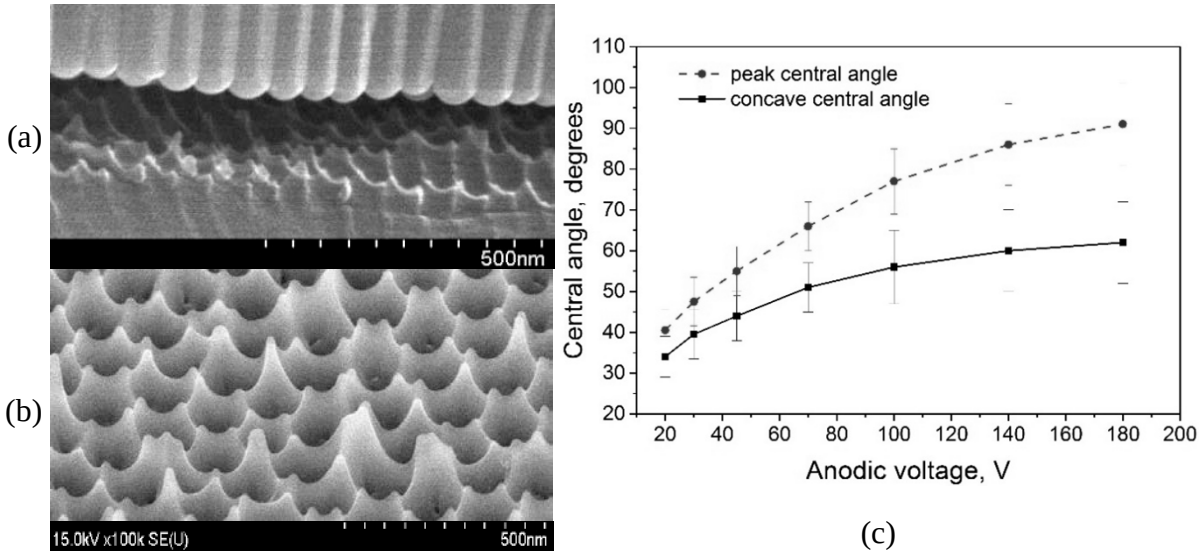

Fig. 5. SEM images of porous alumina and aluminum surface relief formed at different anodic voltages (a) 70, (b) 100 V; central angles *vs* anodic voltage (c)

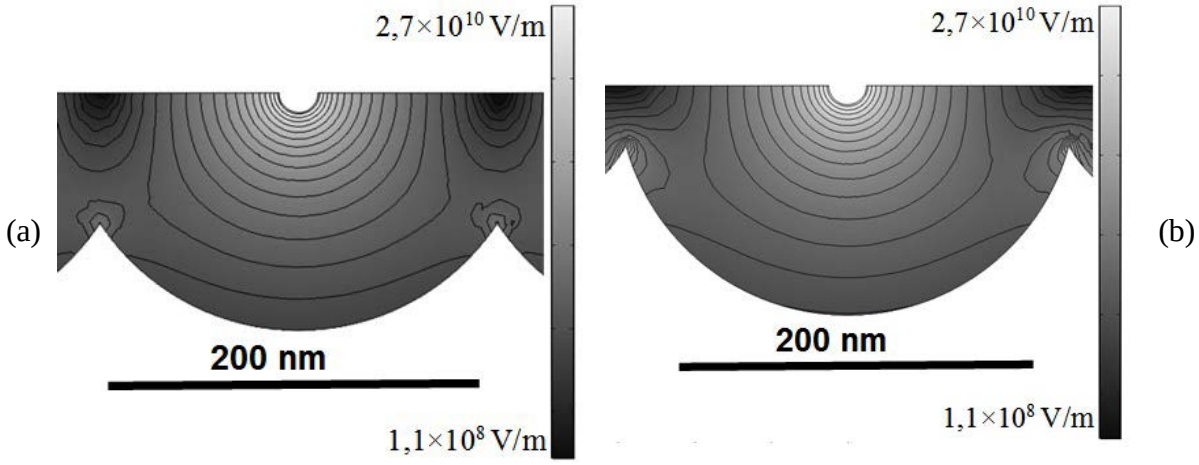

Fig. 6. Electric field distribution in porous alumina cells with different peak central angles: (a) 60, (b) 75 deg. The cells have been formed at U_a=140 V. The lighter areas correspond to the higher electric field strength

The maximum electric field strength surpasses 10^{10} V/m. This value is close to the interatomic electric field of 10^{11} V/m. Such high electric fields can result in impact ionization of aluminum atoms with creation of Al^{3+}- ions near the aluminum peaks. The similar impact ionization of oxygen atoms can occur near the pore bottoms. Thus, we propose that high field nanoplasma regions inside the porous alumina barrier layer are present during the high voltage anodizing process. These nanoplasma regions supply anodizing process with Al^{3+} and O^{2-} ions resulting in appearance of self-organized hexagonal structure and the record anodizing growth rate up to 1 μm/s [4].

Such nanoplasma regions can play the role of self-focusing seeds for pore growth, which ensures the structure self-organization of the growing porous oxide (Fig. 7 a). Note that this phenomenon is analogous to the effect of self-focusing of a light beam in nonlinear optics in an electric field of 10^{10}–10^{11} V/m.

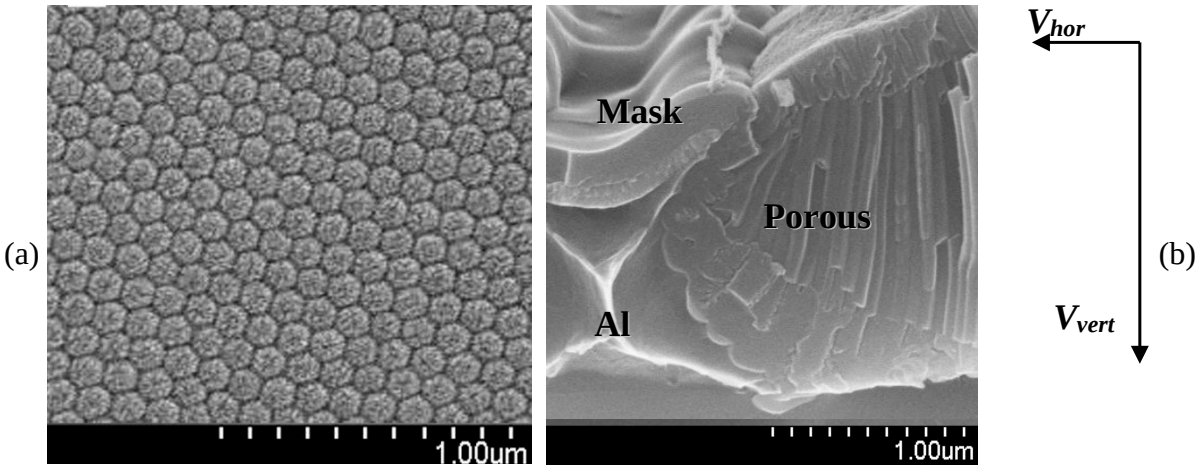

Fig. 7. SEM images of porous alumina: (a) self-ordered frontal surface formed at U_a = 70 V, (b) cross section of porous alumina formed by local anodizing at U_a = 80 V

Another new effect that appears during porous anodizing of aluminum at a high voltage is the anisotropy of anode growth with a masking coating. The anisotropy consists in a noticeable difference between the anodic oxide growth rate in the vertical (V_{vert}) and horizontal (V_{hor}) directions that ensures the minimum lateral shifts during the formation of the pattern specified by a mask (Fig. 7 b). Note that porous anodizing at low voltages is isotropic: the process rate in the horizontal and vertical directions being almost the same [7].

The formation of aluminum interconnections in integrated circuits using porous anodizing of aluminum at a high degree of anisotropy allows using this process for producing VLSI metallization with a submicron element size [9] and opens up new opportunities for the integration of optical and metallic interconnections on silicon chips by planar porous alumina waveguides [10-12]. Another possible application for high field anodizing is to use aluminum surface with high peak central angles for the vertical alignment of liquid crystal materials in display devices [4,13].

Thus, our studies showed that during porous anodizing of aluminum at a high voltage the electric field exceeds 10^{10} V/m in local regions inside oxide that can generate new effects. They include the self-organization of a porous structure, the appearance of nano- and microplasma regions, an anisotropy of porous anodizing. Moreover, other new effects are to be expected during aluminum anodizing under conditions that ensure a high electric field inside the barrier layer of porous oxide.

4. Conclusions

High field porous aluminum anodizing with a photolithographic mask can be carried out in sulfuric acid electrolytes at the highest forming voltage reaching 200 V. It allows obtaining new parameter ranges for the anodic films formed. The central angles of porous alumina can be increased up to 90 deg with the anodic voltage growth. The simulation showed that during anodizing process the electric field strength could exceed 10^{10} V/m in porous alumina nanocells with high central angle values. It allows us to propose the existence of nanoplasma regions near the pore bottom and near aluminum peaks at the border of alumina cells during

high field porous aluminum anodizing. High field anodizing opens new possibilities for porous alumina nanotechnology applications [14].

Acknowledgements. *The authors are grateful to JSC "INTEGRAL" for help with SEM-images.*

References

[1] Thompson G. Porous anodic alumina: fabrication, characterization and applications. *Thin Solid Films.* 1997;297(1-2): 192-201.

[2] Chu S, Wada K, Inoue S, Isogai M, Yasumori A. Fabrication of ideally ordered nanoporous alumina films and integrated alumina nanotubule arrays by high field anodization. *Advanced Materials.* 2005;17(17): 2115-2119.

[3] Yi L, Zhiyuan L, Xing H, Yisen L, Yi C. Formation and microstructures of unique nanoporous AAO films fabricated by high voltage anodization. *Journal of Material Chemistry.* 2011;21(26): 9661-9666.

[4] Lazarouk S, Sasinovich D, Borisenko V, Muravski A, Chigrinov V, Kwok H. Tubular alumina formed by anodization in the meniscal region. *Journal of Applied Physics.* 2010;107(3): 033527.

[5] Li D, Zhao L, Jiang C, Lu J. Formation of anodic aluminum oxide with serrated nanochannels. *Nano Letters.* 2010;10(8): 2766-2771.

[6] Su Z, Zhou W. Pore diameter control in anodic titanium and aluminum oxides. *Journal of Material Chemistry.* 2011;21(2): 357-362.

[7] Lazarouk S, Baranov I, Maello G, Proverbio E, De Cesare G, Ferrari A. Anisotropy of porous anodizing of aluminum for VLSI technology. *Journal of Electrochemical Society.* 1994;141(9): 2556-2559.

[8] Lee K, Tang Y, Ouyang M. Self-ordered, controlled structure nanoporous membranes using constant current anodizing. *Nano Letters.* 2008;8(12): 4624-4629.

[9] Lazarouk S, Katsouba S, Demianovich A, Stanovski V, Voitech S, Vysotski V, Ponomar V. Reliability of built in aluminum interconnection with low-ε dielectric based on porous anodic alumina. *Solid-State Electronics.* 2000;44: 815-818.

[10] Lazarouk S, Leshok A, Katsuba P, Borisenko V. Integration of optical and electronic interconnections on silicon. In: *CriMiCo 2014 - 2014 24th International Crimean Conference Microwave and Telecommunication Technology, Conference Proceedings.* IEEE;2014. p.800-802.

[11] Lazarouk S, Leshok A, Borisenko V, Mazzoleni C, Pavesi L. On the route towards Si-based optical interconnects, Microelectronic Engineering. *Microelectronic Engineering.* 2000;50(1-4): 81-86.

[12] Lazarouk S, Jaguiro P, Leshok A, Borisenko V. Reverse biased porous silicon light-emitting diodes for optical intra-chip interconnects. *Physica E: Low-dimensional Systems and Nanostructures.* 2003;16(3-4): 495-498.

[13] Lazarouk S, Muravski A, Sasinovich D, Chigrinov V, Kwok HS. Porous and pillar structures by anodizing for vertical alignment of nematic liquid crystal. *Japanese Journal of Applied Physics.* 2007;46(10): 6889-6892.

[14] Sousa C, Leitao D, Proenca M, Ventura J, Pereira A, Araujo J. Nanoporous alumina as templates for multifunctional applications. *Applied Physics Review.* 2014;1(3): 031102.